PHYSICAL REVIEW B VOLUME 19, NUMBER 4 15 FEBRUARY 1979

Elastic- and inelastic-neutron-scattering study of tetrathiafulvalenium-tetracyanoquinodimethanide (TTF-TCNQ): New results

J. P. Pouget*
Laboratoire de Physique des Solides associé au Centre National de la Recherche Scientifique, Université Paris-Sud, 91405 Orsay, France

S. M. Shapiro and G. Shirane
Brookhaven National Laboratory, Upton, New York 11973

A. F. Garito and A. J. Heeger
Laboratory for Research on the Structure of Matter, University of Pennsylvania, Philadelphia, Pennsylvania 19174
(Received 4 August 1978)

Several additional studies of tetrathiafulvalenium-tetracyanoquinodimethanide by elastic and inelastic neutron scattering have been performed. The temperature dependence of the lattice parameters b and $a\sin\beta$ were measured and no anomaly was observed at any of the transition temperatures, $T_1 = 54$ K, $T_2 = 48.5$ K, or $T_3 = 38$ K. The $2k_F$ satellites in the $(h\ k\ 0)$ zone have been extensively studied. The temperature dependence of their intensity, position along a^*, and the linewidth along a^* are reported. In contrast with the earlier studies on the $2k_F$ satellites possessing a c^* component, the linewidths of the $(h\ k\ 0)$ satellites increase to above 38 K and the satellites are undetectable above 48 K. The $4k_F$ anomaly is shown not to arise from an anomaly in the longitudinal acoustic branch propagating along b, the chain direction. The possibility of the $4k_F$ anomaly arising from an optical mode or being totally elastic above 54 K cannot be ruled out. The acoustic phonon branches for q propagating along the a^* and c^* directions have been measured and the corresponding elastic constants deduced.

I. INTRODUCTION

The charge-transfer salt, tetrathiafulvalenium-tetracyanoquinodimethanide (TTF-TCNQ), has attracted considerable attention in the past years because of its one-dimensional (1D) electronic properties.[1] After the discovery by x-ray diffuse scattering[2,3] of a $2k_F$ Kohn anomaly, a series of x-ray and neutron-scattering experiments has been performed[4-14] whose synthesis is given in two recent review articles.[15,16]

The situation can be summarized with the aid of Fig. 1. Below the Peierls transition at $T_1 = 54$ K, TTF-TCNQ undergoes two additional transitions at $T_2 = 49$ K and $T_3 = 38$ K. The first-order 38-K transition was first established by neutron-scattering experiments.[4] The 49-K transition was originally predicted from a two-chain Ginsburg-Landau analysis[17] of the initial neutron data and clearly established from additional high-resolution neutron-scattering experiments.[9-13] Other anomalies have been observed in the vicinity of these phase transitions.[18,19] At 54 K, the $2k_F$ anomaly is partially condensed giving a $2a \times 3.4b \times c$ modulated structure with the appearance of new satellites at $\vec{q} = (0.5a^*, 0.295b^*, 0)$. Below 49 K, the a component of this structure begins to vary until $T_3 = 38$ K when there is a lock-in transition to the $4a \times 3.4b \times c$ modulated structure.

In the dynamical studies,[7] a phonon anomaly at $2k_F = 0.29b^*$ in the transverse acoustical (TA) branch polarized along c^* was found to develop below 150 K. Its 1D character was unambiguously established by further x-ray investigations[8] which also revealed a new 1D precursor at the wave vector $0.59b^*$. This was interpreted as $4k_F$ scattering reflecting the strong interactions between the electrons.[20] This new anomaly, polarized along the stacking b direction, was observed by x-ray scattering up to room temperature.[10,12] The x-ray studies[12] also showed that below 150 K, the diffuse scattering at $2k_F$ possessed a longitudinal component[21] in addition to the transverse component observed by neutron scattering. The dynamical origin of this longitudinal component is currently unknown.

This sequence of phase transitions has been approached theoretically in terms of various two-chain models in which the two different types of stacks become modulated either at different temperatures[18,22] or at the same temperature, but with different amplitudes.[23] It was also suggested[12,15] on the basis of x-ray photographs, that the 54 K phase transition is due to the condensation of the $2k_F$ transverse anomaly, while the 49 K phase transition corresponds to the condensation of both longitudinal anomalies at $2k_F$ and $4k_F$. However, a clear confirmation of the sequence of the distortions of the different stacks must await the structural determinations of the distorted low-temperature phases.

Being far from a complete determination, the

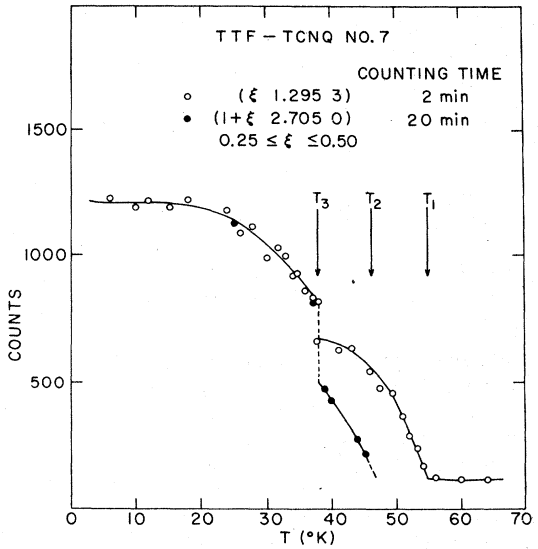

FIG. 1. Temperature of two different satellites. Also shown are the three phase-transition temperatures [taken from Comès *et al.* (Ref. 5)].

understanding of the exceptional properties of TTF-TCNQ has progressed only by the limited studies in a few Brillouin zones where the effects are the strongest. In this spirit, the purpose of this paper is to present new investigations of the structural properties of TTF-TCNQ by neutron scattering in order: (i) to collect additional $2k_F$ satellites in the three low temperature modulated phases, particularly those coming from the condensation of the longitudinal part of the $2k_F$ anomaly; (ii) to study the dynamical origin of the $4k_F$ anomaly; (iii) to improve our knowledge on the lattice dynamics of this compound by measuring the low lying phonon branches.

The format of this paper is as follows. All the experimental details are given in Sec. II. Elastic neutron scattering measurements on the $2k_F$ longitudinal satellites are presented in Sec. III. Inelastic scattering studies are given in Sec. IV, in which the status of the search for the dynamical origin of the $4k_F$ anomaly will be presented and some new low lying-phonon branches reported. Finally, Sec. V will summarize the results obtained.

II. EXPERIMENTAL

The neutron-scattering experiments were performed on the triple-axis spectrometers at the Brookhaven High Flux Beam Reactor using 13.5- or 14.8-meV incoming neutrons and pyrolytic graphite as monochromator, analyzer, and filter. The triple-axis elastic configuration was used for high-$\vec{Q}$ resolution, with the analyzer set to remove the inelastic background and to improve the resolution.

The deuterated single crystals of TTF-TCNQ are those used in the earlier experiments. Sample $N7$ (fully characterized in Ref. 7) is formed by an assembly of 17 almost untwinned crystals. It was mounted in the $(0hl)$ zone. Samples A and B, larger (volume ~0.02 cm^3) and irregular in shape, were mounted in the $(0hl)$ and $(hk0)$ zones, respectively.

The elastic measurements have been exclusively performed with the best sample $N6$, which was already used in the high resolution elastic studies reported in Ref. 9 and 13. This sample, approximately $25 \times 2 \times 0.05$ mm in size, was wrapped in aluminum foil and mounted strain-free in the $(hk0)$ zone.

An early x-ray measurement of the lattice parameters of TTF-TCNQ gave indications of an anomaly near 55 K.[24] We report below measurements of the temperature dependence of the lattice parameters of the deuterated strain-free sample $N6$. The lattice parameters $a \sin\beta$ amd b were obtained by measuring the positions of the (300) and (020) Bragg reflection and their temperature dependence is shown in Fig. 2. The temperature variation is smooth and no anomalies observed at T_1, T_2, or T_3. The linewidth was determined by the resolution of our instrument and showed no variation with temperature. The lattice parameter b, directed along the stacking direction exhibits a large dilation on heating corresponding to 2%

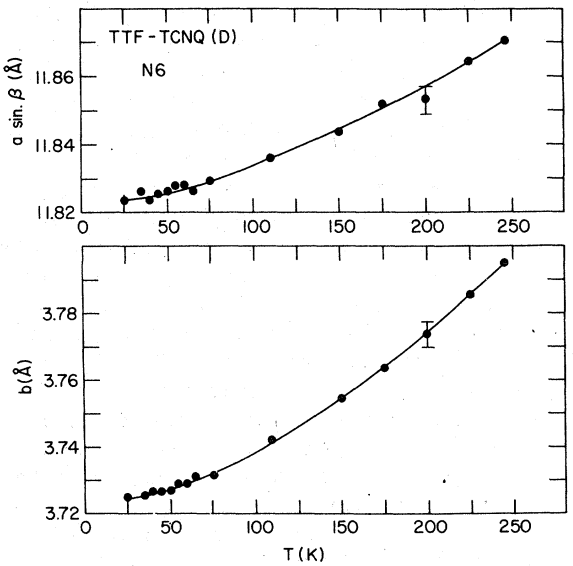

FIG. 2. Temperature variation of the $a \sin\beta$ and b parameters of deuterated TTF-TCNQ.

change between 25 and 250 K as already noted from the x-ray and thermal-expansion studies.[24,25] It should be noted that the value of the lattice parameters obtained in the present experiment on deuterated samples are in good agreement with those obtained in the x-ray studies on protonated samples. This, and the fact that the transition temperatures appear to be the same for the protonated and deuterated samples, imply that the hydrogens play only a minor role in the phase transitions.

III. $2k_F$ SATELLITES IN THE ($hk0$) BRILLOUIN ZONES

The early elastic neutron scattering measurements[4,5,9,13] showed that the strongest $2k_F$ satellites were in the (013) and (113) Brillouin zones. With a non-zero l index, these satellites come (partly at least) from the condensation, below 54 K, of the transverse acoustical $2k_F$ anomaly. However, such is not the case for the very weak $(1+q_a\,2.705\,0)$ satellite observable below 45 K as shown in Fig. 1. An interesting aspect of this satellite is that its peak intensity seems to extrapolate to zero near T_2. A previous x-ray study[15] showed that the condensed satellites possess both a longitudinal and transverse component. However, with the l index equal zero only the longitudinal part of the $2k_F$ anomaly is probed. On these bases, Khanna *et al.*[12] have suggested that the longitudinal part of the $2k_F$ anomaly condenses at T_2 whereas the transverse part condenses at $T_1 = 54$ K. In this section we report on more extensive studies of the temperature dependence of the longitudinal $2k_F$ satellites present in the ($hk0$) Brillouin zones.

In Table I are listed the additional satellites that were observable at 25 K. The squares of the structure factors F^2_{obs}, relative to F^2_{obs} of the (300) Bragg peak are also given. It can be seen that

TABLE I. Structure factor of observed $2k_F$ satellites in the ($hk0$) zones, at 25 K, relative to F^2_{obs} (300) Bragg peak.

h	k	l	F^2_{obs}
3	0	0	100 000
0	2	0	14 750
0.25	0.705	0	17
0.75	0.705	0	17
0.25	1.295	0	3
1.25	1.295	0	5
0.25	1.705	0	15
0.25	2.295	0	22
3.25	2.295	0	17
0.75	2.705	0	25
1.25	2.705	0	15

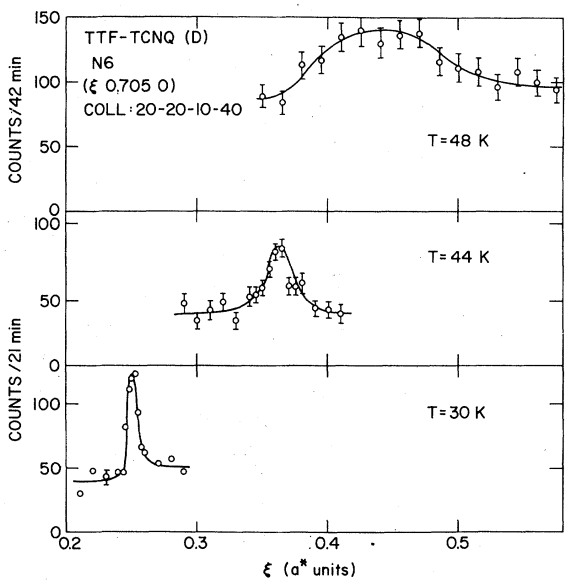

FIG. 3. Elastic scans along the a^* direction showing the $2k_F$ satellite (q_a 0.705 0) at 30, 44, and 48 K.

the strongest intensities correspond to the (0.25 0.705 0) and (0.75 0.705 0) satellite positions. In the present study, the intensity, position and linewidth along the a^* direction of these two satellites have been studied as a function of temperature. Additional measurements have also been performed with the (1.25 2.705 0) satellite in order to give a

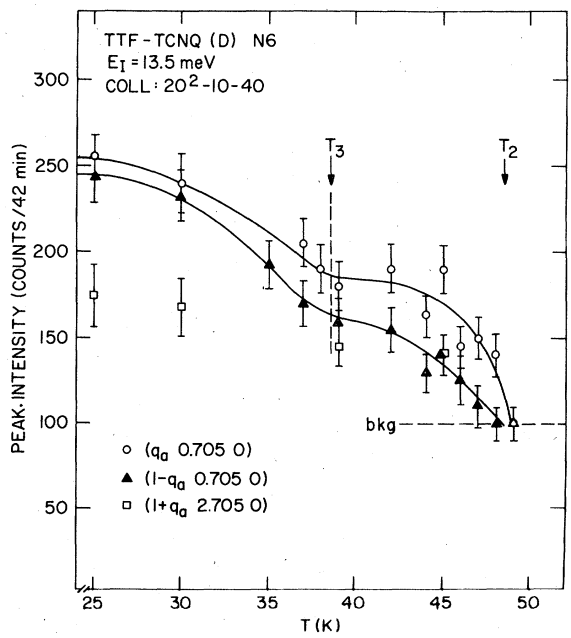

FIG. 4. Temperature variation of the peak intensity of the (q_a 0.705 0), ($1-q_a$ 0.705 0), and ($1+q_a$ 2.705 0) satellites. The temperature corresponding to the 38-K (T_3) and 49-K (T_2) phase transitions is indicated.

comparison with the earlier published data.[5] Finally, all the data reported here have been taken on heating, because, as studied in detail by Ellenson *et al.*[13] with the (q_a 1.295 3) satellite, the position and even the linewidth of the satellites in the intermediate modulated phase depend upon whether the temperature at which the measurement is done was reached by heating or cooling.

Typical profiles of the (q_a 0.705 0) satellite in the a^* direction are given in Fig. 3 for several temperatures. The temperature variation of the peak intensity of the three satellites studied is given in Fig. 4. Their peak intensities decrease with increasing temperature as reported earlier in the (1-q_a 2.705 0) satellite. The strongest satellite (q_a 0.705 0) remains observable up to 48 K (see Fig. 3), but at 49 K it is no longer distinguishable above the background. Finally, from Fig. 4, the ratio of the peak intensity to the background is about $\frac{3}{2}$ for the satellite at (1 + q_a 2.705 0) at T = 39 K, which is consistent with the earlier results [see the satellite profile presented for the same sample in Fig. 6(c) in Ref. 5].

In the temperature range where the longitudinal $2k_F$ satellites are observable, the temperature variation of the modulation along a^* was measured. This quantity is shown in Fig. 5 and is in good agreement with the previous measurements of the stronger satellites measured about (013).[9,13]

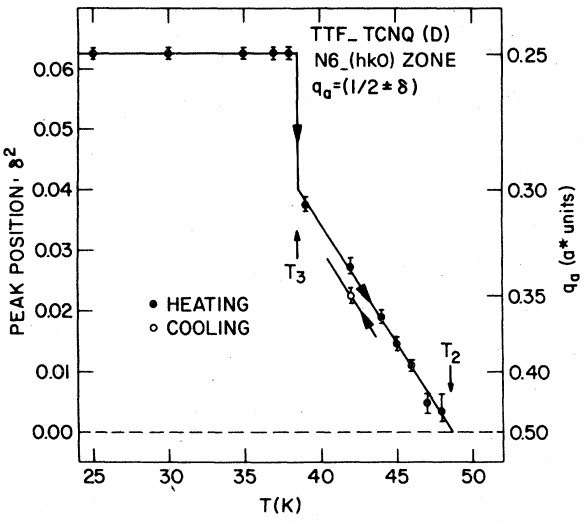

FIG. 5. Plot of the $2k_F$ satellite positions along a^*, measured upon heating for the satellites present in the (hk0) zones. The functional relationship between δ^2 (left-hand scale) and q_a (right-hand scale) is given in the heading. One satellite position measured upon cooling is also presented to show in the intermediate phase the constant hysteresis of 1 K between the heating and cooling curves. The two temperatures T_2 and T_3 indicated are taken from the data upon heating.

T_2 = 48.5 is determined by extrapolating the linear part of the curve to δ = 0. The same thermal hysteresis observed on cooling in a prior experiment[13] is also present in these satellites. It is important to note that in contrast to those satellites measured about (013), the satellites measured in the (hk0) Brillouin zone, i.e., no component along c, are not observable between T_2 and T_1. This is consistent with the x-ray results of Khanna *et al.*[12]

Figure 6 shows the temperature variation of the full width at half-maximum (FWHM) for the two "longitudinal" $2k_F$ satellites studied. It is only below 38 K, in the lower modulated phase, that their linewidth is resolution limited. On heating, these satellites seem to disappear due to divergence of their linewidth, but the integrated intensity remains temperature independent, within experimental errors. For comparison, Fig. 6 also shows the linewidth of the (q_a 1.295 3) satellite taken from the original data of Ellenson *et al.*[13] on the same sample mounted in a different zone. Although broadened, the (q_a 1.295 3) satellite is visible up to T_1. Its broadening, however, is smaller and less temperature dependent than that of the (q_a 0.705 0) and (1-q_a 0.705 0) satellites.

The temperature-dependent broadening of the linewidth along a^* is most likely due to a decrease

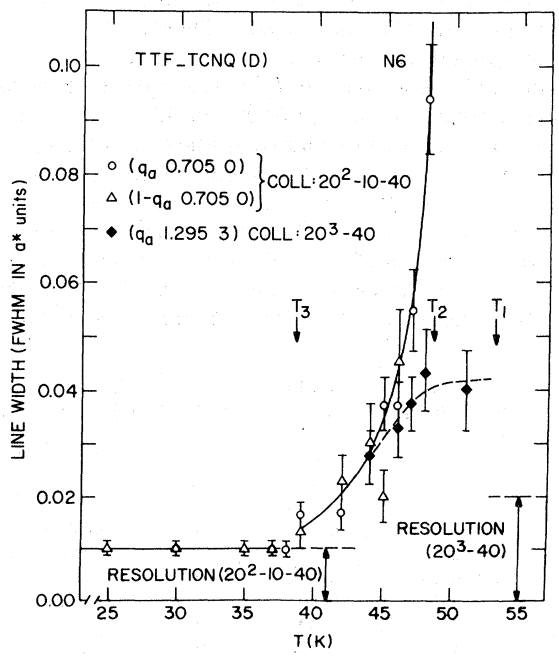

FIG. 6. FWHM measured upon heating along the a^* direction for the (q_a 0.705 0), (1 − q_a 0.705 0), and (q_a 1.295 3) satellites. The three temperatures corresponding to the 38-K (T_3), 49-K (T_2), and 54-K (T_3) phase transitions are indicated.

of the correlation length between the TTF and TCNQ stacks. This incomplete order above 38 K raises the same questions asked for potassium cyanoplatinate (KCP)[25-27] concerning the effects of impurities, lattice defects, or intrinsic phase fluctuations in the condensation of the $2k_F$ anomaly. More puzzling are the two different transverse correlation lengths observed above 45 K (Fig. 6). Are we observing the development of two different types of short-range order due to noncoupled degrees of freedom (one degree of freedom corresponding to the longitudinal $2k_F$ anomaly and the other to the transverse $2k_F$ anomaly)? Is there a development of a different kind of order within each kind of stack (e.g., the transverse anomaly corresponding to the TCNQ stacks and the longitudinal anomaly for the TTF stacks)?

IV. INELASTIC SCATTERING

A. Inelastic behavior near $4k_F$

The $4k_F$ anomaly in TTF-TCNQ, first discovered by x-ray diffuse scattering,[8] has generated considerable interest, and many theories[20] have been proposed to explained the origin of this scattering. Roughly speaking, these theories predict either an inelastic (phonon-anomaly) or an elastic (static charge density waves in 1D Wigner lattices) origin for this scattering.

Further x-ray experiments[10,12] have found that the $4k_F$ scattering is visible up to room temperature and is mainly polarized along the stacking b direction. Therefore, we performed detailed measurements of the longitudinal acoustical (LA) branch near the zone boundary, especially around the $\vec{q}=1-4\vec{k}_F=0.45b^*$ at room temperature and $\vec{q}=0.41b^*$ at 150 K. Most of the measurements have been performed near the zone boundary in the ω-q range defined by the outline in Fig. 7(a). As already demonstrated in the case of $2k_F$ anomalies in KCP (Ref. 26) and TTF-TCNQ,[7] the best way to visualize this anomaly is to give the distribution of the cross section in the ω-q plane. This leads to the intensity contour plots shown in Fig. 7(b) for the data taken at 295 K in the (013) Brillouin zone. This figure and a similar plot realized from the measurements in the (002) zone show clearly that no anomalous dispersion of the LA branch near $q=4k_F$ is present at room temperature. The data taken in both zones at 150 K also lead to the same conclusion. (The limit of our

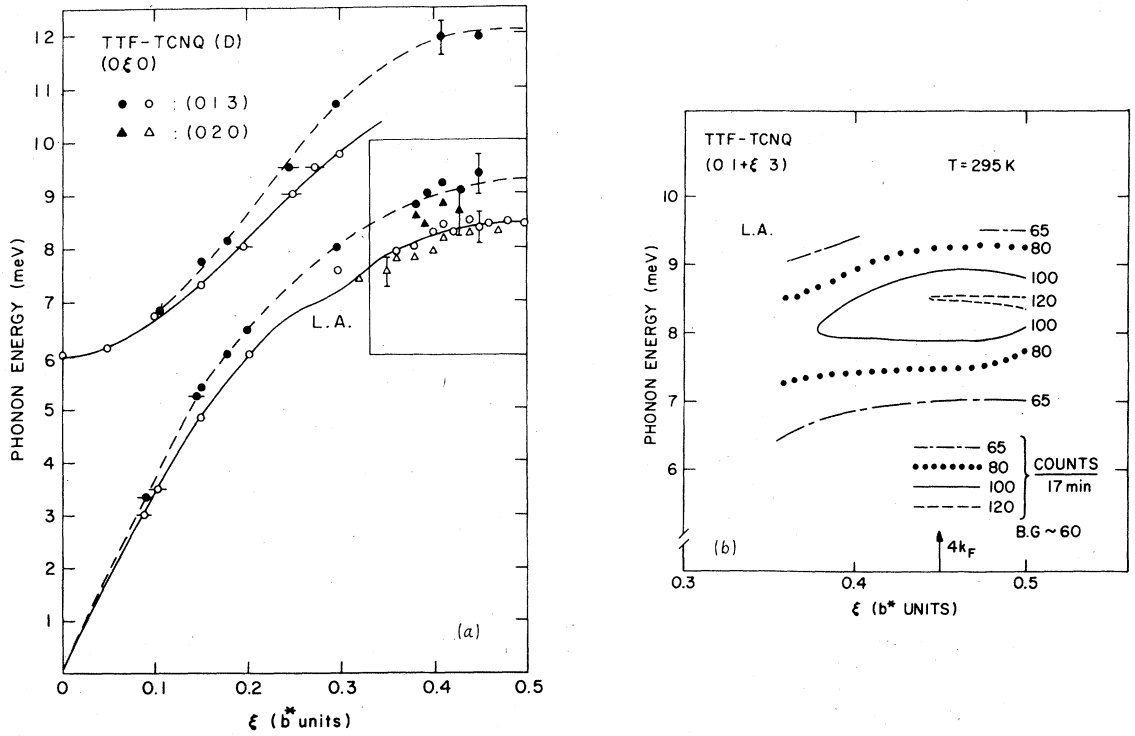

FIG. 7. (a) Dispersion curves for the longitudinal acoustical and a low-lying optical modes propagating along the [010] chain direction in TTF-TCNQ at 150 K (full symbols—dashed line) and 295 K (open symbols—solid line). The solid line for the LA branch is from Ref. 7. (b) Contour intensity plot around the $1-4k_F$ position in ω-q range shown by the outline in (a).

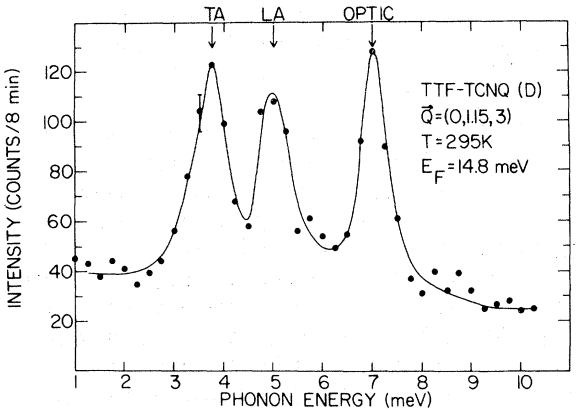

FIG. 8. Energy scan at room temperature for $\xi = 0.15$ in the (013) Brillouin zone showing the relative strength of the transverse acoustical, longitudinal mode, and optical mode.

detectability is about 2 counts/min). Moreover, Fig. 7(a) shows clearly that the frequency of the longitudinal branch increases on cooling.

Several elastic studies around the $4k_F$ position have been performed at room temperature in several Brillouin zones in the $(0kl)$ scattering plane. No evidence of $4k_F$ scattering has been observed. However, it must be remarked that with the high background level present (10 counts/min) a weak anomaly [comparable in intensity to that observed at $2k_F$ in the TA(c^*) mode[7]] might not be detected under the present conditions. Similar elastic scans performed at 150 K have led to the same conclusion. Thus we can eliminate the possibility that a strong anomaly (yielding more than 2 counts/min) exists in the LA branch but a similar anomaly in the elastic scattering cannot be ruled out. Another possibility, not explored in detail because of the limited sample size, is that the $4k_F$ anomaly arises from an optical mode that has an anomaly at $q = 4k_F$.

Within the (013) Brillouin zone we were able to measure one of the low-lying optical modes and its dispersion is shown in Fig. 7. No anomaly is seen at $q = 4k_F$. Figure 8 shows a typical spectrum. By comparison of the intensities of the three features, we see that the dynamical structure factor for this mode is large in the (013) zone. This can be explained by the in-phase scattering of molecules possessing the same angle of tilt [the scattering vector (013) is roughly perpendicular to the plane of the molecules].

B. Dispersion curves for phonons propagating along the a^* and c^* direction

At room temperature we also measured the dispersion curves of the acoustic modes propagating along the a^* and c^* directions, and the results are shown in Figs. 9 and 10. Because of the monoclinic symmetry only the TA modes polarized

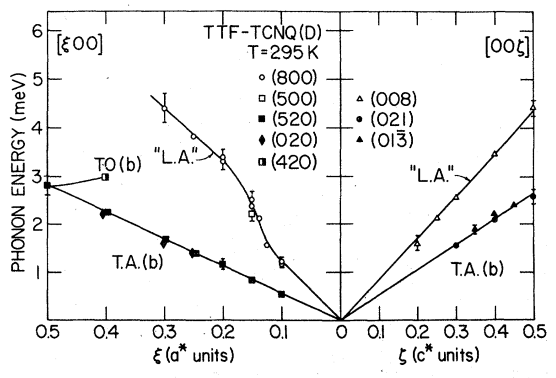

FIG. 9. Dispersion curves of some low-lying modes propagating along the a^* and c^* direction for TTF-TCNQ at room temperature.

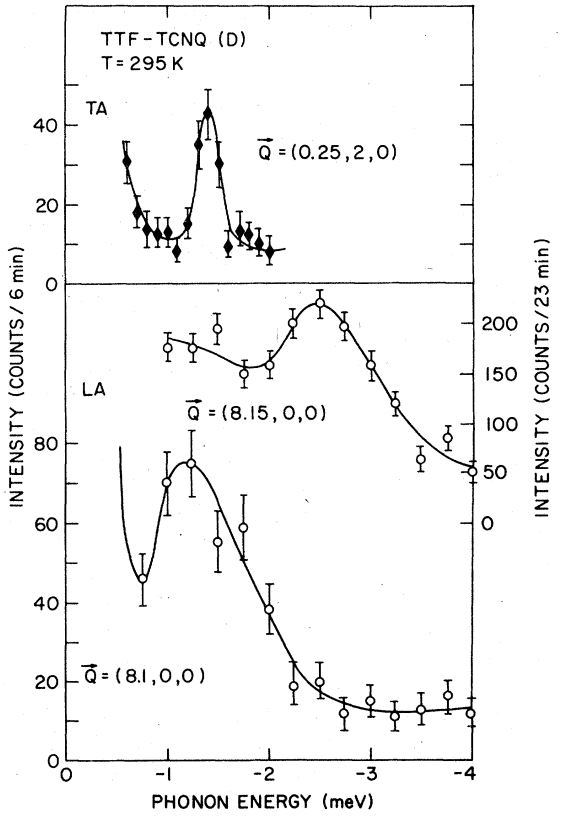

FIG. 10. Room-temperature spectra of the transverse and "longitudinal" acoustical mode propagating along the a^* direction showing particularly the anomalous increase of the frequency of the "longitudinal" branch between $\xi = 0.10$ and $\xi = 0.15$.

TABLE II. Effective elastic constants C_{eff}, deduced from the sound velocity V_s, of the dispersion curve for acoustical phonons of wave vector $\hat{q}$ and polarization $\hat{e}$ in TTF-TCNQ at 295 K.

Mode	$\hat{q}$	$C_{\text{eff}} = \rho v_s^2$	$\hat{e}$	(10^{11} dyn/cm^2)	References
"LA"	[100]	2.0 ± 0.4	≃[100]	($\simeq C_{11}$)	This work
TA	[100]	0.42 ± 0.03	[010]	($= C_{66}$)	This work
TA	[010]	0.42 ± 0.07	≃[100]	($\simeq C_{66}$)[a]	11
LA	[010]	1.7 ± 0.3	[010]	($= C_{22}$)	7
TA	[010]	0.88 ± 0.12	≃[001]	($\simeq C_{44}$)[a]	7
TA	[001]	0.87 ± 0.08	[010]	($\simeq C_{44}$)[a]	This work
"LA"	[001]	2.2 ± 0.4	≃[001]	($\simeq C_{33}$)	This work

[a] Using the exact expressions $\frac{1}{2}\{(C_{66}+C_{44}) + [(C_{66}-C_{44})^2 + 4C_{46}^2]^{1/2}\}$ for $\hat{e} \simeq [100]$, $\frac{1}{2}\{(C_{66}+C_{44}) - [(C_{66}-C_{44})^2 + 4C_{46}^2]^{1/2}\}$ for $\hat{e} \simeq [001]$, and $C_{66}\cos^2\beta + C_{44}\sin^2\beta - C_{46}\sin 2\beta$ for $\hat{e} = [010]$, one gets with the monoclinic angle $\beta = 104.5°$, $C_{44} = (0.88 \pm 0.22) \times 10^{11}$ dyn/cm^2 and $C_{46} = (0.04 \pm 0.60) \times 10^{11}$ dyn/cm^2.

along b are purely transverse. The "longitudinal" modes are not purely longitudinal and may contain a small transverse component. The space group of TTF-TCNQ is $P2_1/c$ which has a glide plane along the c direction, the direction of like molecular stacks, giving a $2c^*$ pseudoperiodicity along c^*. This is why the acoustical modes of Fig. 9 have a finite slope at the zone boundary at $0.5c^*$.

Along the a^* direction, a gap is expected at the zone boundary, but it must be small since within our resolution the gap is not observed (Fig. 9). The TO modes shown in Fig. 9 is a continuation of the TA mode into the next Brillouin zone and corresponds to an out of phase motion of the TTF and TCNQ sheets along the b direction. The "LA" mode propagating along a^* shows an anomalous dispersion between $q = 0.10$ and $q = 0.15$ as seen in Fig. 9 and in the spectra of Fig. 10. This could be due to a coupling with a low-lying optical mode.

From the initial slope of the acoustic modes it is possible to calculate an effective elastic constant: $C_{\text{eff}} = \rho v_s^2$ where $\rho = 1.62$ g/cm^3 is the density of TTF-TCNQ and v_s is the velocity of sound. The elastic constants obtained from Fig. 9 and Refs. 7 and 11 are given in Table II along with the particular C_{ij}. Table II shows that within error $C_{11} \approx C_{22} \approx C_{33}$, which is surprising for such an anisotropic system. C_{11} and C_{33} are also 50% lower than the elastic constants deduced from high-pressure compressibility measurements.[28] C_{44} and C_{66} exhibit significant anisotropy and are in agreement with the earlier measurement of the transverse modes propagating along b^*.[11]

V. SUMMARY

New information on the structural properties of TTF-TCNQ has been obtained during this study:

No anomaly of the lattice parameters has been observed at the three low-temperature phase transitions.

The $2k_F$ satellites in the $(hk0)$ Brillouin zones arising from the condensation of the longitudinal part of the $2k_F$ anomaly have been studied. They correspond to the same modulation of the lattice as the $2k_F$ satellites originating in the condensation of the $2k_F$ transverse acoustical (c^* polarization) anomaly. The main difference between the transverse and longitudinal satellites is that the linewidth along a^* of the latter grows rapidly above T_3 so that the longitudinal satellite is not observable above T_2.

The $4k_F$ anomaly is not present in the LA branch and any elastic $4k_F$ scattering must be weaker than the anomaly associated with $2k_F$.

Several acoustical branches for q propagating along the $\vec{a}^*$ and $\vec{c}^*$ directions have been measured. The slope at the origin of the TA(b^*) branch is consistent with that reported in the earlier measurements of the TA(c^*) and TA(a^*) branches for q propagating along $\vec{b}^*$. Surprisingly, no anisotropy is observed in the slope of the LA modes propagating along the a^*, b^*, c^* directions.

ACKNOWLEDGMENTS

We would like to thank Paul Nigrey for growing the deuterated samples used in this study. We also benefited from discussions with R. Comès, W. D. Ellenson, and V. J. Emery. Research at BNL was supported by the Division of Basic Energy Sciences, U.S. Dept. of Energy, under Contract No. EY-76-C-02-0016. Research at the Laboratory for Research on the Structure of Matter, University of Pennsylvania, was supported in part by the NSF and Advanced Research Projects Agency.

*Guest scientist at BNL.
[1]*Low Dimensional Cooperative Phenomena*, edited by H. J. Keller (Plenum Press, New York, 1975); *One-Dimensional Conductors*, Lecture Notes in Physics, Vol. 34 (Springer, New York, 1975); A. J. Berlinsky, Contemp. Phys. 17, 331 (1976); J. J. André, A. Bieber, and F. Gautier, Ann. Phys. (N. Y.) 1, 145 (1976); *Chemistry and Physics of One-Dimensional Metals*, edited by H. J. Keller (Plenum Press, New York, 1977); *Organic Conductors and Semi-conductors*, Lectures Notes in Physics (Springer, New York, 1976), Vol. 65.
[2]F. Denoyer, R. Comès, A. F. Garito, and A. J. Heeger, Phys. Rev. Lett. 35, 445 (1975).
[3]S. Kagoshima, H. Anzai, K. Kajimura, and R. Ishigoro, J. Phys. Soc. Jpn. 39, 1143 (1975).
[4]R. Comès, S. M. Shapiro, G. Shirane, A. F. Garito, and A. J. Heeger, Phys. Rev. Lett. 35, 1518 (1975).
[5]R. Comès, G. Shirane, S. M. Shapiro, A. F. Garito, and A. J. Heeger, Phys. Rev. B 14, 2376 (1976).
[6]H. A. Mook and C. R. Watson, Phys. Rev. Lett. 36, 801 (1976).
[7]G. Shirane, S. M. Shapiro, R. Comès, A. F. Garito, and A. J. Heeger, Phys. Rev. B 14, 2325 (1976).
[8]J. P. Pouget, S. K. Khanna, F. Denoyer, R. Comès, A. F. Garito, and A. J. Heeger, Phys. Rev. Lett. 37, 437 (1976).
[9]W. D. Ellenson, R. Comès, S. M. Shapiro, G. Shirane, A. F. Garito, and A. J. Heeger, Solid State Commun. 20, 53 (1976).
[10]S. Kagoshima, T. Ishiguro, and H. Anzai, J. Phys. Soc. Jpn. 41, 2061 (1976).
[11]S. M. Shapiro, G. Shirane, A. F. Garito, and A. J. Heeger, Phys. Rev. B 15, 2413 (1977).
[12]S. K. Khanna, J. P. Pouget, R. Comès, A. F. Garito, and A. J. Heeger, Phys. Rev. B 16, 1468 (1977).
[13]W. D. Ellenson, S. M. Shapiro, G. Shirane, and A. F. Garito, Phys. Rev. B 16, 3244 (1977).
[14]H. A. Mook, G. Shirane, and S. M. Shapiro, Phys. Rev. B 16, 5233 (1977).
[15]R. Comès, in *Chemistry and Physics of One-Dimensional Metals*, edited by H. J. Keller (Plenum, New York, 1977), p. 315.
[16]R. Comès and G. Shirane, in *Highly Conducting One-Dimensional Solids*, edited by J. T. Devreese (Plenum, New York, to be published).
[17]P. Bak and V. J. Emery, Phys. Rev. Lett. 36, 978 (1976).
[18]D. Jérome, W. Müller, and M. Weger, J. Phys. (Paris) Lett. 35, L77 (1974).
[19]R. A. Craven, M. B. Salamon, G. Depasqualt, R. M. Herman, G. D. Stucky, and A. Schultz, Phys. Rev. Lett. 32, 769 (1974); A. J. Schultz, G. D. Stucky, R. A. Craven, N. Y. Schaffman, and M. B. Salamon, J. Am. Chem. Soc. 98, 5191 (1976); D. Djurek, K. Franulovic, M. Prester, S. Tomic, L. Giral, and J. M. Fabre, Phys. Rev. Lett. 38, 715 (1977).
[20]V. J. Emery, Phys. Rev. Lett. 37, 107 (1976); J. B. Torrance, in *Chemistry and Physics on One-Dimensional Metal*, edited by H. J. Keller (Plenum, New York, 1977), p. 137; P. A. Lee, T. M. Rice, and R. A. Klemm, Phys. Rev. B 15, 2984 (1977); J. Kondo and K. Yamaji, J. Phys. Soc. Jpn. 43, 424 (1977); J. Hubbard, Phys. Rev. B 17, 494 (1978).
[21]Here we discard the very weak $2k_F$ scattering observed by x-ray scattering at room temperature (Refs. 3, 10, 12) which can be related to the weak shallow phonon anomaly found in the longitudinal acoustical branch (Ref. 7).
[22]T. D. Schultz and S. Etemad, Phys. Rev. B 13, 4928 (1976); P. Bak, Phys. Rev. Lett. 37, 1077 (1976); A. Bjelis and S. Barisic, *ibid.* 37, 1517 (1976); D. Mukamel, Phys. Rev. B 16, 1741 (1977); B. Horovitz and D. Mukamel, Solid State Commun. 23, 285 (1977).
[23]E. Abrahams, J. Solyom, and F. Woynarovich, Phys. Rev. B 16, 5238 (1977).
[24]A. J. Schultz, G. D. Stucky, R. B. Blessing, and P. Coppens, J. Am. Chem. Soc. 98, 3194 (1976).
[25]D. E. Schafer, G. A. Thomas, and F. Wudl, Phys. Rev. B 12, 5532 (1975).
[26]K. Carneiro, G. Shirane, S. A. Werner, and S. Kaiser, Phys. Rev. B 13, 4258 (1976).
[27]B. Renker, L. Pintschovius, W. Glaser, H. Retschel, R. Comès, L. Liebert, and W. Drexel, Phys. Rev. Lett. 32, 836 (1974); J. W. Lynn, M. Iizumi, G. Shirane, S. A. Werner, and R. B. Saillant, Phys. Rev. B 12, 1154 (1975).
[28]D. Debray, R. Millet, D. Jérome, S. Barisic, J. M. Fabre, and L. Giral, J. Phys. (Paris) Lett. 38, 227 (1977).